

# Preparation and mechanical performance of Cf-SiCf-(Al<sub>2</sub>O<sub>3p</sub>) reinforced geopolymer composites

Shu Yan<sup>1,2</sup>, Peigang He<sup>1,2,\*</sup>, Dechang Jia<sup>1,2</sup>, Jinyan Wang<sup>1,2</sup>, Zhihua Yang<sup>1,2</sup>, Xiaoming Duan<sup>1,2</sup>, and Yu Zhou<sup>1,2</sup>

<sup>1</sup>Institute for Advanced Ceramics, Harbin Institute of Technology, Harbin 150080, China

<sup>2</sup>School of Materials Science and Engineering, Harbin Institute of Technology, Harbin 150080, China

**Abstract.** The C<sub>f</sub>-SiC<sub>f</sub>-(Al<sub>2</sub>O<sub>3p</sub>)/KGP composites were successfully prepared by the method that mixing a kind of hybrid fiber preform pre-developed and geopolymer resin. The synergistic effects of the hybrid fibers and Al<sub>2</sub>O<sub>3</sub> particles on the composites were investigated. Results show that all the composites showed typical amorphous structure. Mechanical properties of the C<sub>f</sub>-SiC<sub>f</sub>-(Al<sub>2</sub>O<sub>3p</sub>)/KGP composites were improved remarkably due to the addition of the hybrid fibers and Al<sub>2</sub>O<sub>3</sub> particles. The flexural strength and Young's modulus of the C<sub>f</sub>-SiC<sub>f</sub>-Al<sub>2</sub>O<sub>3p</sub>/KGP composites with 1 mm length SiC<sub>f</sub> were reached 62.4±2.1 MPa and 24.1±1.6 GPa, respectively. The C<sub>f</sub>-SiC<sub>f</sub>-(Al<sub>2</sub>O<sub>3p</sub>)/KGP composites showed non-catastrophic behavior rather than the catastrophic failure.

## 1 Introduction

Geopolymers are an novel three-dimensional inorganic aluminosilicate polymers which synthesis by aluminosilicate source materials under highly alkaline conditions [1-4]. Geopolymers offer variety of characteristics and properties, such as low densities, low costs, easy processing and fire resistance, thus attract lots of industrial attentions [1-7]. However, the pure geopolymers showed disadvantages of both low mechanical performance and catastrophic fracture behavior, thus limits its applications as structural components [1-7]. In recent years, many studies have been explored on geopolymer matrix composites to overcome the disadvantages of itself low strength and brittle failure, including nanotube [8,9], graphene [10-11], particles [12-13], short fiber [14-16,20] and continuous fiber [17-19]. Ranjbar [19] evaluated fiber-matrix interaction and mechanical properties of two different fibers (polypropylene (PPF) and micro steel fibers (MSF)) reinforced fly ash based geopolymer. Results show that MSF has strong contact with the matrix because it tends to behave as a hydrophilic material, while PPF led to fiber-matrix debonding due to hydrophobic characteristics. Timakul et al [20] reported the addition of basalt fibers into the fly ash-based geopolymer can improve its compressive strength. Lin et

\* Corresponding author: peiganghe@hit.edu.cn

al. [14, 21-22] prepared the short carbon fiber geopolymer matrix composites using sheet-like fiber preform, and improved the mechanical properties. The addition of  $\alpha$ -Al<sub>2</sub>O<sub>3</sub> particles into the composites could reduce the volume change of the composites and improve the mechanical properties, especially at high temperatures [22].

In our previous research, we have attempted short carbon fiber and SiC fiber reinforced geopolymer composites, respectively [21-22, 23]. The short carbon fiber reinforced showed good mechanical properties with non-brittle failure behavior [21]. The SiC fiber exhibited similar mechanical properties as carbon fiber, and much higher oxidation resistance [24], which makes it a prominent high-temperature reinforcing candidate. However, compared with the carbon fibers, the SiC fiber is much expensive. Thus, it inspired us to introduce C<sub>f</sub>, SiC<sub>f</sub> and Al<sub>2</sub>O<sub>3</sub> particles into the geopolymer to improve the mechanical properties.

In this study, we provided a simple method to prepare C<sub>f</sub>-SiC<sub>f</sub>-(Al<sub>2</sub>O<sub>3p</sub>)/KGP composites. The synergistic effects of the hybrid fibers and Al<sub>2</sub>O<sub>3</sub> particles on the composites were investigated. The microstructure and the mechanical properties of the composites were also studied.

## 2 Materials and experiments

The composition of the geopolymer matrix was SiO<sub>2</sub>/Al<sub>2</sub>O<sub>3</sub> = 4.0, K<sub>2</sub>O/SiO<sub>2</sub> = 0.3 and H<sub>2</sub>O/K<sub>2</sub>O = 11 (mole ratio) according our previous work [17, 22]. The raw materials were KOH (Tianjin Guangfu Indus., China), silica sol (Jiangsu Xiagang, Indus., China), kaolin (95%, Fengxian Reagent Factory, China) and  $\alpha$ -Al<sub>2</sub>O<sub>3p</sub>(Xiamen Fushixin Indus., China). The kaolin was heated treated at 800 °C for 2 h to get the metakaolin powder. Carbon fiber(Jilin Carbon Indus., China) used in this study has a diameter of 6-8 $\mu$ m and an average tensile strength of 3 GPa. SiC fiber (Jiangsu Sailifei Ceramic Fiber Indus., China) has a diameter of 13  $\mu$ m and an average tensile strength of 1.5-1.6 GPa. The properties of Carbon and SiC fibers were shown in Table 1. SiC fiber used in this study was first treated at 370 °C in an air atmosphere for 2 h to remove the surface epoxy coating [25].

The alkaline solution was obtained by mixing KOH and silica sol for 3 days using magnetic stirring. Whereafter, the Al<sub>2</sub>O<sub>3</sub> particle (the ratio of Al<sub>2</sub>O<sub>3</sub>/metakaolin was 0.75 wt.%) was added to geopolymer resin and mixed homogeneously. The composites were prepared by infiltrating geopolymer resin into the short carbon fiber and SiC fiber preform with the help of the ultrasonic vibration treatment, and stacked one by one to get a green sample with 20 layers. The carbon fiber content was 4.5 vol%, and fiber length was 7 mm. The SiC fiber content was also 4.5 vol%, and fiber length was 1, 3 and 5 mm. To remove the pores in the composites, degassing was applied at 70 °C for 3 days using a vacuum-bag technique after mechanical pressing.

**Table 1.** Properties of Carbon and SiC fiber

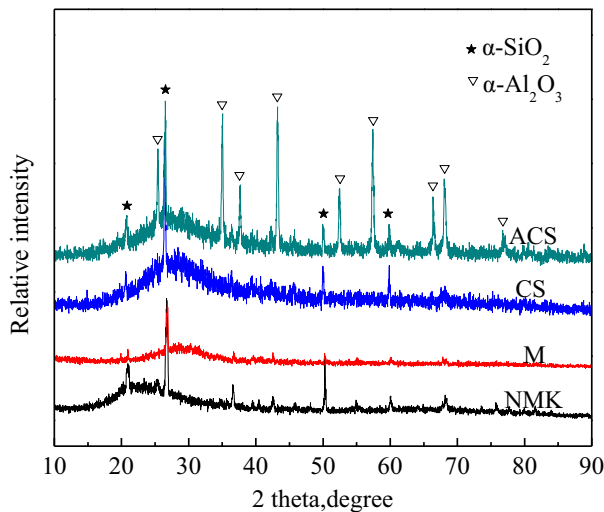
| Brand                     | Density (g•cm <sup>-3</sup> ) | Diameter ( $\mu$ m) | Tensile strength (GPa) | Modulus (GPa) | Elongation (%) |
|---------------------------|-------------------------------|---------------------|------------------------|---------------|----------------|
| C <sub>f</sub> -TX-3      | 1.76                          | 6~7                 | ≥3.0                   | 210~230       | ≥1.4           |
| SiC <sub>f</sub><br>SLFC1 | 2.36                          | 13±0.5              | 1.5~1.6                | 140±10        | 1.3~1.4        |

The phases of C<sub>f</sub>-SiC<sub>f</sub>-(Al<sub>2</sub>O<sub>3</sub>) reinforced geopolymer composites were characterized using an X-ray diffractometer (XRD: Rigaku, D/MAX-2200VPC, Tokyo, Japan) with CuK $\alpha$  radiation at a scan rate of 4°/min. Mechanical properties of the composites in the x direction(in-plane and perpendicular to fiber axial direction) and z direction (laminare lay-up direction) were investigated. Flexural strength measurements were conducted on

specimens( $3 \times 4 \times 36 \text{ mm}^3$ ) using a three-point-bending fixture on an Instron-500 testing machine with a span length of 30 mm at a crosshead speed of 0.5 mm/min. Work of fracture was calculated by the area between load curves and x axis in the load/displacement curves till the load dropped to 90% of the maximum load. Five to six specimens were tested under each test condition. Surface micrographs of the  $C_f\text{-SiC}_f\text{-(Al}_2\text{O}_3)$  reinforced geopolymer composites were observed by optical microscope. Fractographs of the composites were observed by scanning electron microscopy.

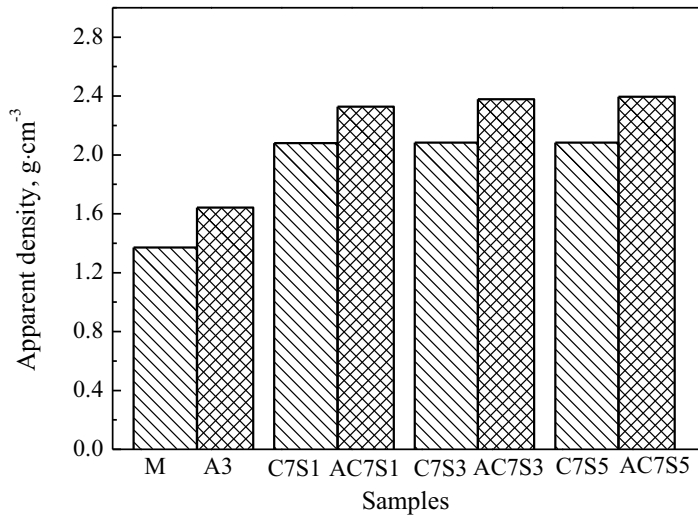
### 3 Results and discussions

Fig. 1 shows the XRD patterns of the metakaolin, pure geopolymer matrix,  $C_f\text{-SiC}_f/\text{KGP}$  and  $C_f\text{-SiC}_f\text{-Al}_2\text{O}_{3p}/\text{KGP}$  composites. Metakaolin particles showed characteristic amorphous hump between  $22^\circ 2\theta$ , and several reflections from quartz present introduced by the raw kaolin [17]. The pure geopolymer matrix displayed typical broad amorphous humps around  $28^\circ 2\theta$ . The characteristic amorphous hump of the  $C_f\text{-SiC}_f/\text{KGP}$  composites was similar to the pure geopolymer matrix, but shifted to a lower position around  $27^\circ$ . The addition of  $C_f$  and  $\text{SiC}_f$  seems to retard the geopolymerization process of the matrix [25]. However, with the addition of  $\text{Al}_2\text{O}_{3p}$ , typical  $\text{Al}_2\text{O}_3$  peaks in  $C_f\text{-SiC}_f\text{-Al}_2\text{O}_{3p}/\text{KGP}$  composites was observed, indicating the incorporation of  $\text{Al}_2\text{O}_{3p}$  may not participate in the geopolymerization process of the matrix.



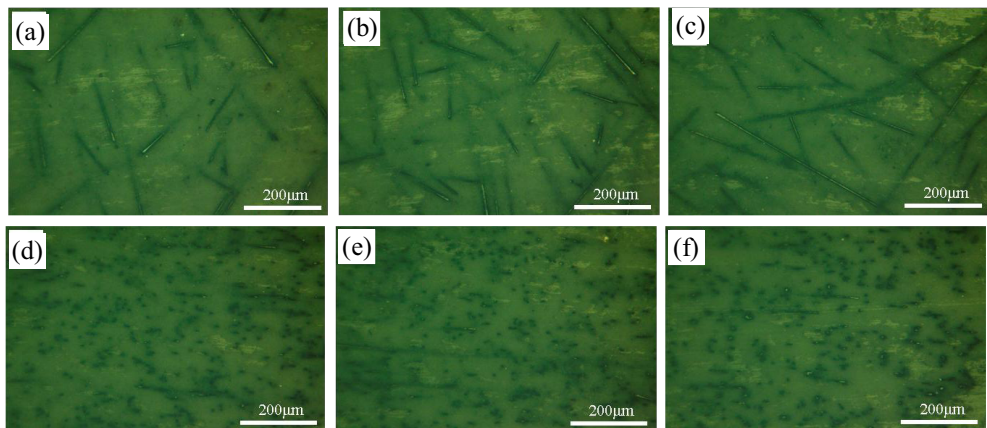
**Fig. 1.** XRD patterns of metakaolin, geopolymer matrix  $C_f\text{-SiC}_f/\text{KGP}$  and  $C_f\text{-SiC}_f\text{-Al}_2\text{O}_{3p}/\text{KGP}$  composites

Fig.2 shows the density data of the  $C_f\text{-SiC}_f\text{-(Al}_2\text{O}_{3p})/\text{KGP}$  samples. The density of the geopolymer matrix was  $1.37 \text{ g}\cdot\text{cm}^{-3}$ . The addition of the  $C_f$  and  $\text{SiC}_f$  increased the density of the composites, while there was no obvious difference between the samples with different fiber length. The addition of the  $\alpha\text{-Al}_2\text{O}_{3p}$  obviously increased the density of the composites. The density of the  $C_f\text{-SiC}_f/\text{KGP}$  and  $C_f\text{-SiC}_f\text{-(Al}_2\text{O}_{3p})/\text{KGP}$  were  $2.08 \text{ g}\cdot\text{cm}^{-3}$  and  $2.38 \text{ g}\cdot\text{cm}^{-3}$ , respectively.



**Fig. 2.** the Density data of the C<sub>f</sub>-SiC<sub>f</sub>-(Al<sub>2</sub>O<sub>3p</sub>)/KGP samples

With the help of the ultrasonic scattering treatment, it can effectively prevent fibers from too much aggregation. All the composites showed homogeneous microstructure, most short carbon fibers own a two-dimension in geopolymer matrix, as shown in Fig. 3.



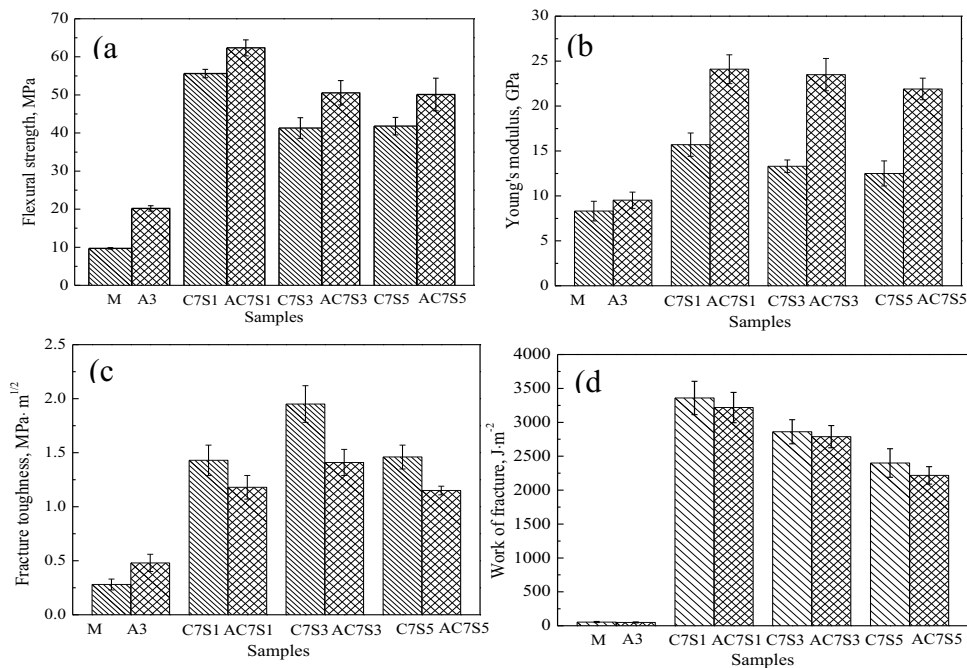
**Fig. 3.** Micrographs of the surface of C<sub>f</sub>-SiC<sub>f</sub>/KGP composites (a)-(c) Surface micrographs of C7S1, C7S3 and C7S5, (d)-(f) Cross-section micrographs of C7S1, C7S3 and C7S5

Table 2 shows the mechanical properties of the C<sub>f</sub>-SiC<sub>f</sub>-(Al<sub>2</sub>O<sub>3p</sub>)/KGP composites. With the cooperation of hybrid fibers, the flexural strength and Young's modulus of the composites improved significantly. It should be pointed out that with Al<sub>2</sub>O<sub>3p</sub> addition, the flexural strength and Young's modulus of the corresponding composites were increased than before, indicating the significant strengthening effect from Al<sub>2</sub>O<sub>3p</sub>. There was no obvious difference of the mechanical properties between x direction and z direction. Fig.4 shows the mechanical properties of the C<sub>f</sub>-SiC<sub>f</sub>-(Al<sub>2</sub>O<sub>3p</sub>)/KGP composites in x direction. The flexural strength for the composites ramped up first, reached the peak value when SiC fiber length was 1 mm, and then decreased with longer fiber length. The flexural strength of the C<sub>f</sub>-SiC<sub>f</sub>-Al<sub>2</sub>O<sub>3p</sub>/KGP composites was higher than the C<sub>f</sub>-SiC<sub>f</sub>/KGP samples, reached the

peak value of  $62.4 \pm 2.1$  MPa for the AC7S1 sample, which was 6.4 times as high as that of geopolymer matrix ( $9.7 \pm 0.2$  MPa) and then decreased for the composite with the length of SiC<sub>f</sub> fiber increased.

**Table 2.** Mechanical properties of the Cf-SiCf-(Al<sub>2</sub>O<sub>3</sub>p)/KGP composites

| Samples | Flexural strength (MPa) |             | Young's modulus (GPa) |             | Fracture toughness (MPa·m <sup>1/2</sup> ) | Work of fracture (J·m <sup>-2</sup> ) |
|---------|-------------------------|-------------|-----------------------|-------------|--|---------------------------------------|
|         | x direction             | z direction | x direction           | z direction |  |                                       |
| M       | 9.7±0.2                 | 9.7±0.2     | 8.31±0.1              | 8.31±0.1    | 0.28±0.05                                  | 54.2±8.1                              |
| C7S1    | 55.6±1.1                | 60.8±1.3    | 15.7±1.3              | 19.0±0.5    | 1.43±0.14                                  | 3359.1±245.8                          |
| C7S3    | 41.3±2.7                | 50.2±4.5    | 13.3±0.7              | 10.4±0.7    | 1.95±0.17                                  | 2860.9±178.2                          |
| C7S5    | 41.8±2.3                | 42.5±1.0    | 12.5±1.4              | 8.2±0.3     | 1.46±0.11                                  | 2399.7±211.3                          |
| A3      | 20.2±0.7                | 20.2±0.7    | 9.53±0.9              | 9.53±0.9    | 0.48±0.08                                  | 48.7±7.2                              |
| AC7S1   | 62.4±2.1                | 60.9±3.4    | 24.1±1.6              | 27.8±0.4    | 1.18±0.11                                  | 3218.1±223.8                          |
| AC7S3   | 50.6±3.2                | 53.0±2.1    | 23.5±1.8              | 27.3±2.2    | 1.41±0.12                                  | 2788.5±163.9                          |
| AC7S5   | 50.1±4.3                | 47.2±2.3    | 21.9±1.2              | 22.3±1.6    | 1.15±0.04                                  | 2217.46±129.4                         |



**Fig. 4.** Mechanical properties of the C<sub>f</sub>-SiC<sub>f</sub>-(Al<sub>2</sub>O<sub>3</sub>p)/KGP composites in x direction (a) Flexural strength, (b) Young's modulus, (c) Fracture toughness, (d) work of fracture

Similarly, compared with the geopolymer matrix, the Young's modulus of the  $C_f$ - $SiC_f$ - $(Al_2O_{3p})/KGP$  composites showed increased with the incorporation of fiber and  $Al_2O_3$  particles. the Young's modulus also reached the peak value of  $24.1 \pm 1.6$  GPa for AC7S1, which was 2.9 times as high as that of the geopolymer matrix ( $8.31 \pm 0.1$  GPa), which shows a significant synergistic strengthening effect of the  $Al_2O_3$  particles and fibers. With the increase in SiC fiber length, the Young's modulus of both the  $C_f$ - $SiC_f/KGP$  and  $C_f$ - $SiC_f$ - $Al_2O_{3p}/KGP$  composites decreased.

While, the toughness effect of  $Al_2O_{3p}$  on the fracture toughness and work of fracture of the composites were not always positive. Fig. 4c and d show the fracture toughness and the work of fracture of the  $C_f$ - $SiC_f$ - $(Al_2O_{3p})/KGP$  composites. The fracture toughness of the  $C_f$ - $SiC_f/KGP$  composites reached the peak value when SiC<sub>f</sub> length was 3 mm, and then decreased for the composites with a longer fiber length of 5 mm. The addition of the  $Al_2O_{3p}$  increased the fracture toughness of the geopolymer matrix, from  $0.28 \pm 0.05$  to  $0.48 \pm 0.08$   $MPa \cdot m^{1/2}$ , rising by 71.4%. However, compared with the  $C_f$ - $SiC_f/KGP$ , within the SiC fiber was 1,3 and 5, the fracture toughness of the  $C_f$ - $SiC_f$ - $Al_2O_{3p}/KGP$  composites decreased by 17.4%, 27.7% and 21.2%, respectively. When fiber fiber was 1mm, the composite exhibited the highest work of fracture,  $3359.1 \pm 245.8 J \cdot m^{-2}$ , which was 61 times as high as that of pristine geopolymer. The work of fracture of the  $C_f$ - $SiC_f$ - $Al_2O_{3p}/KGP$  composites was much lower than the  $C_f$  and  $SiC_f$  reinforced ones. This may due to the addition of the  $Al_2O_{3p}$  may increase the viscosity of the slurry and bring some defects and pores, which was sensitive to cracks [22, 26].

Fig.5 shows the stress and displacement curves of  $C_f$ - $SiC_f$ - $(Al_2O_{3p})/KGP$  composites in x direction. The pure geopolymer matrix indicated a typical brittle failure mode, while all the composites showed non-catastrophic ones with the presence of both elastic region and nonlinear region. After stress reached the maximum values, the strength tended to reduce slowly and several significant steep drop-steps, especially for the C7S3 and AC7S3 samples, corresponding to interface debonding, fiber fracturing and pulling-out [23, 25].

The typical fractographs of the  $C_f$ - $SiC_f$ - $(Al_2O_{3p})/KGP$  composites were studied, as shown in Figs. 6. There was no obvious difference between the composites with and without  $Al_2O_3$  particles. As for the composites, fiber fracturing and lots of fiber pulling-out could be seen on the fracture surface, which were due to the weak bonding strength between the fiber and the geopolymer matrix [14, 27]. They are all helpful to consume much higher fracture energy and enhance the fracture toughness of the composites [14, 27]. This ensured the effective toughening and could prevent the catastrophic fracture of the composites, which make the composites presents typical non-catastrophic behavior.

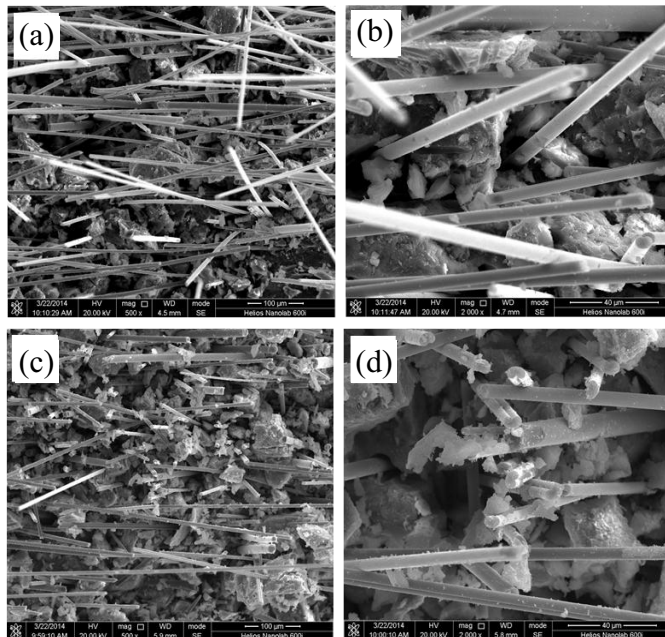


**Fig. 5.** Fractograph of the (a)-(b)  $C_F-SiC_F/KGP$  and (c)-(d)  $C_F-SiC_F-Al_2O_{3p}/KGP$  composites

## 4 Conclusions

In the present study,  $C_F-SiC_F-(Al_2O_{3p})/KGP$  composites with different silicon carbide fiber lengths and fixed carbon fiber lengths were prepared by the method that mixing a kind of hybrid fiber preform pre-developed and geopolymer resin. The synergistic effects of the hybrid fibers and  $Al_2O_3$  particles on the on the microstructure and mechanical properties of the composites are studied.

The  $C_F-SiC_F-(Al_2O_{3p})/KGP$  composites showed typical amorphous structure and most short carbon fibers own a two-dimension in geopolymer matrix. The addition of the  $\alpha-Al_2O_{3p}$  obviously increased the density of the composites. The density of the  $C_F-SiC_F/KGP$  and  $C_F-SiC_F-(Al_2O_{3p})/KGP$  were approximate  $2.08 g \cdot cm^{-3}$  and  $2.38 g \cdot cm^{-3}$ , respectively.

Mechanical properties of the  $C_F-SiC_F-(Al_2O_{3p})/KGP$  composites were improved remarkably due to the addition of the hybrid fibers and  $Al_2O_3$  particles. The flexural strength and Young's modulus were enhanced further with the incorporation of  $Al_2O_{3p}$ . Compared with the geopolymer marix, the flexural strength and Young' s modulus of the  $C_F-SiC_F-Al_2O_{3p}/KGP$  composites with 1mm length  $SiC_F$  were increased 5.4 times and 1.9 times, respectively. All the  $C_F-SiC_F-(Al_2O_{3p})/KGP$  composites showed non-catastrophic behavior rather than the catastrophic failure. Fiber fracturing and lots of fiber pulling-out the fracture surface of the composites contributed to the enhancement of the toughness and work of fracture of the composites.

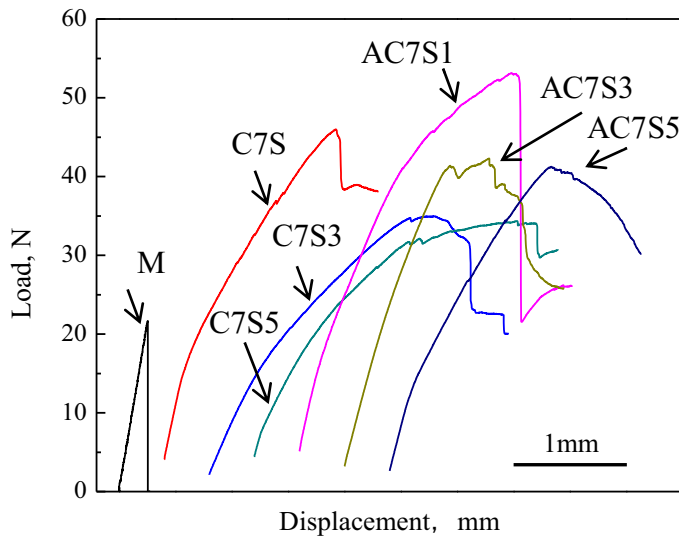


**Fig. 6.** Stress and displacement curves of SiCf/KGP composites in x direction.

This work was supported by the Fundamental Research Funds for the Central Universities (Grant no. HITNSRIF20165), and the National Natural Science Foundation of China (NSFC, Nos.51372048, 51502052, 51321061 and 51225203).

## References

- 1 J. Davidovits, *J. Therm. Anal.*, **37**, 1633 (1991)
- 2 K. Komnitsas, D. Zaharaki, *Miner. Eng.*, **20**, 1261 (2007)
- 3 D. Khale, R. Chaudhary, *Mater. Sci.*, **42**, 729 (2007)
- 4 K.J.D. MacKenzie, *Ceram. Trans.*, **153**, 175 (2003)
- 5 M.M.A. Abdullah, K. Hussin, M. Bnhussain, K.N. Ismail, W.M.W. Ibrahim, *Int. J. Pure Appl. Sci. Technol.*, **6**, 35 (2011)
- 6 J. Feng, R. Zhang, L. Gong, Y. Li, W. Cao, X. Cheng, *Mater. Des.*, **65**, 529 (2015)
- 7 J Tailby, K.J.D. MacKenzie, *Cem. Concr. Res.*, **40**, 787 (2010)
- 8 K.J.D. MacKenzie, M.J. Bolton, *J. Mater. Sci.*, **44**, 2851 (2009)
- 9 H.M.M. Khater, H.A.A. Gawwad, *Epitoanyag*, **2**, 38 (2015)
- 10 N. Ranjbar, M. Mehrali, M. Mehrali, U.J. Alengaram, M.Z. Jumaat, *Cem. Concr. Res.*, **76**, 222 (2015)
- 11 M. Saafi, L. Tang, J. Fung, M. Rahman, F. Sillars, J. Liggat, X. Zhou, *Smart Mater. Struct.*, **23**, 065006 (2014)
- 12 E. Kamseu, A. Rizzuti, C. Leonelli, D. Perera, *J. Mater. Sci.*, **45**, 1715 (2010)
- 13 S.A. Bernal, J. Bejarano, C. Garzon, R. Mejía de Gutiérrez, S. Delvasto, E. D. Rodríguez, *Compos. Part B: Eng.*, **43**, 1919 (2012)
- 14 T. Lin, D. Jia, P. He, M. Wang, D. Liang, *Mater. Sci. Eng., A*, **497**, 181 (2008)
- 15 Z. Yunsheng, S. Wei, Z. Li, X. Zhou, *ACI Mater. J.*, **106**, 3 (2009)
- 16 V. Dhand, G. Mittal, K.Y. Rhee, S.J. Park, D. Hui, *Composites Part B*, **73**, 166 (2015)
- 17 P. He, D. Jia, T. Lin, M. Wang, Y. Zhou, *Ceram. Int.*, **36**, 1447 (2010)
- 18 Q. Zhao, B. Nair, T. Rahimian, P. Balaguru, *J. Mater. Sci.*, **42**, 3131 (2007)
- 19 N. Ranjbar, S. Talebian, M. Mehrali, C. Kuenzel, H.S.C. Metselaar, M.Z. Jumaat, *Compos. Sci. Technol.*, **122**, 73 (2016)
- 20 P. Timakul, W. Rattanaprasit, P. Aungkavattana, *Ceram. Int.*, **42**, 6288 (2016)

- 21 T. Lin, D. Jia, M. Wang, P. He, D. Liang, Bull. Mater. Sci., **32**, 77 (2009)
- 22 T. Lin, D. Jia, P. He, M.R. Wang, Journal of Central South University of Technology, **16**, 881 (2009)
- 23 J. Yuan, P. He, D. Jia, S. Yan, D. Cai, L. Xu, Z. Yang, X. Duan, S. Wang, Y. Zhou, Ceram. Int., **42**, 5345 (2016)
- 24 B. Liang, Z. Yang, Y. Li, J. Yuan, D. Jia, Y. Zhou, Ceram. Int., **41**, 8868 (2015)
- 25 P. He, D. Jia, B. Zheng, S. Yan, J. Yuan, Z. Yang, X. Duan, J. Xu, P. Wang, and Y. Zhou, Ceram. Int., **42**, 12239 (2016)
- 26 H. Li, H. Xiao, J. Ou, Cem. Concr. Res., **34**, 435 (2004)
- 27 T. Lin, D. Jia, P. He, M. Wang, Mater. Sci. Eng., A **527**, 2404 (2010)